JOURNAL OF SOLID STATE CHEMISTRY **135,** 103–110 (1998)
ARTICLE NO. SC977604

Synthesis and Crystal Structure of the Vacancy-Ordered $LaNi_{1-x}M_xO_{2.5+\delta}$ (M = Mn, Fe, Co) Phase

Siv Aasland,*[,1] Helmer Fjellvåg,*[,2] and Bjørn C. Hauback†

*Department of Chemistry, University of Oslo, N-0315 Oslo, Norway; and †Institutt for Energiteknikk, N-2007 Kjeller, Norway

Received March 3, 1997; in revised form August 19, 1997; accepted August 21, 1997

The synthesis and crystal structure of a new type of oxygen-deficient compound with the formula $LaNi_{1-x}M_xO_{2.5+\delta}$ (M = Mn, Fe, Co) are reported. The new phases crystallize in a tetragonal cell with dimensions $a_T = 2\sqrt{2}\,a_C$ and $c_T = a_C$, where a_C means the cell parameter of an ideal cubic perovskite. The structure was refined in space group $P4/m$ ($Z = 8$), with deficiency of four oxygen atoms per unit cell, i.e., $La_8(Ni_{1-x}M_x)_8O_{20}$, compared to the ideal perovskite. The crystal structure and the ordering of the oxygen vacancies were determined by synchrotron powder X-ray and neutron powder diffraction. The structure is built of corner-sharing NiO_6 octahedra, NiO_5 pyramids, and NiO_4 square-planar groups with La^{3+} occupying ten-coordinated voids.

INTRODUCTION

Nonstoichiometry in metal oxides adopting the perovskite structure has been a subject of detailed studies during the past several decades (1–3). The ideal ABO_3 perovskite structure consists essentially of a framework of corner-sharing BO_6 octahedra, with the large A cation occupying a void of about the same size as the oxygen atom. Ordering of oxygen vacancies in the ABO_{3-x} defect pervoskites results in large supercells of the aristotype (3). The type of superstructure formed depends mainly on the nature of the B cation.

Vacancy ordering in oxygen-deficient $LaNiO_3$ was first observed by Gai and Rao (4), who suggested the formation of a series of phases with the general formula $La_nNi_nO_{3n-1}$. The structure of oxygen-deficient $LaNiO_{3-x}$ was later studied by a number of authors (5–10). Alonso and Martinez-Lope recently solved the structure of $LaNiO_{2.5}$ ($n = 2$ in the series $La_nNi_nO_{3n-1}$) from neutron powder diffraction data (10). $LaNiO_{2.5}$ was indexed on a monoclinic cell with $a = 7.8386(2)$ Å, $b = 7.7969(2)$ Å, $c = 7.4674(2)$ Å and $\beta = 93.841(2)^\circ$. The crystal structure is a monclinically distorted $2 \times 2 \times 2$ perovskite-type superstructure. The oxygen vacancies are ordered in such a way that square-planar NiO_4 and NiO_6 octahedra alternate in the ab plane along the [110] direction. The ordered oxygen-deficient $La_nNi_nO_{3n-1}$ phases could not be prepared by ordinary solid-state reactions and were instead prepared from the perovskite $LaNiO_3$ by a topotactic reduction either in a reducing atmosphere or by Zr metal in sealed ampules (5, 11). Vidyasagar *et al.* similarly synthesized the $LaCoO_{2.5}$ phase by a topotactic reduction of $LaCoO_3$ (7). Recently, neutron powder diffraction data showed that $LaCoO_{2.5}(La_2Co_2O_5)$ has an orthorhombic cell [$a = 5.4439(1)$ Å, $b = 15.8704(4)$ Å, $c = 5.6924(1)$ Å] with a brownmillerite structure involving alternate sheets of CoO_6 octahedra and CoO_4 tetrahedra along the b axis (12). The crystal structure is a $\sqrt{2} \times 2 \times \sqrt{2}$ superstructure of the perovskite type. A series of $La_nMn_nO_{3n-1}$ phases formed during the reduction of perovskites of the type $LaMnO_{3+x}$ were observed by Abbattista and Borlera (13). The crystal structure of $La_nMn_nO_{3n-1}$ was suggested to involve sequences of $n-1$ MnO_6 octahedral sheets alternating with MnO_4 tetrahedral sheets. No such ordered oxygen-deficient structures have, to the authors' knowledge, been reported in the $LaFeO_{3-x}$ system. However, oxygen-deficient perovskites containing copper and lanthanum have been extensively studied during the past years owing to their potential features as high-T_c superconductors. A number of ordered oxygen-deficient phases have been found: $(La,Sr)_8Cu_8O_{20}$ (14), $(La,Sr)_5Cu_5O_{13}$ (15), $(La,Sr)_4Cu_4O_{10}$ (16), and $(La,Sr)_8Cu_8O_{16+\delta}$ (17). In these structures, copper is found in four-, five-, and six-coordinated environments.

In the present paper, a structural study of the series $LaNi_{1-x}M_xO_{2.5+\delta}$ (M = Mn, Fe, Co) was undertaken to examine the influence of small substitutions of other transition metals for nickel in the ordered oxygen-deficient $LaNiO_{2.5}$ ($La_2Ni_2O_5$) phase. The new compounds were prepared by a topotactic reduction of the perovskite $LaNi_{1-x}M_xO_3$ (M = Mn, Fe, Co) phases using Zr metal as oxygen scavenger, and the crystal structures were studied by powder X-ray and neutron diffraction.

[1]Present address: SINTEF Materials Technology, Sem Sælandsv. 12, N-7034 Trondheim, Norway.

[2]To whom correspondence should be addressed.

0022-4596/98 $25.00

EXPERIMENTAL

Starting materials for the syntheses were La_2O_3 (99.99%, Molycorp), $Mn(CH_3COO)_2 \cdot 4H_2O$ (> 99%, Fluka), Fe (99.999%, Koch-Light Ltd.), $Co(CH_3COO)_2 \cdot 4H_2O$ (> 99%, Fluka), $Ni(CH_3COO)_2 \cdot 4H_2O$ (> 99%, Fluka), citric acid monohydrate [$C_3H_4(OH)(COOH)_3 \cdot H_2O$] (reagent grade, Sturge Biochemicals), and HNO_3 (p.a., Merck). Prior to use, the La_2O_3 was heated to 1273 K to remove any hydrated and/or carbonated species. The actual metal contents of the acetates (Mn, Co, Ni) were determined gravimetrically. La_2O_3 and Fe were first dissolved in diluted HNO_3; thereafter the metal acetates and excess citric acid were added to the solution. After complete dissolution of the citric acid, the solution was heated on a hot plate to remove water and nitric oxides, and the liquid turned into a glassy gel. The gel was dried at 450 K and crushed before most of the carbonaceous species were removed by incineration at 720 K for a few hours. The sample was then ground in an agate mortar and pressed into pellets, which were placed in an alumina crucible and heated at 1073 K under flowing O_2 for 1 week with one intermittent grinding. The resulting perovskites $LaNi_{1-x}M_xO_3$ (M = Mn, Fe, Co), $0 \leq x \leq 0.25$, were all found to have the rhombohedral structure reported for pure $LaNiO_3$ (18).

The perovskites were reduced to the nominal composition $LaNi_{1-x}M_xO_{2.5}$ with appropriate amounts of Zr metal in quartz ampules which were evacuated and sealed. The ampules were placed in a furnace with a thermal gradient giving a sample temperature of 673 K and a temperature close to the Zr metal of 873 K. After 7–15 days the quartz ampule was quenched in a bucket of ice and water. The ampule was transferred to an Ar-filled glovebox (< 1 ppm O_2 and H_2O) and opened carefully.

The oxygen contents of the reduced perovskite samples were determined thermogravimetrically by completely reoxidizing the samples. 50–100 mg of each sample was transferred directly from the glovebox in an alumina crucible and heated to 800 K at a heating rate of 5 K min^{-1} in air in a Perkin-Elmer TGA7 system. The analyzed oxygen contents are all slightly greater than 2.50 ($\delta > 0$) (Table 1). This may indicate incomplete oxidation of zirconia, an extreme tendency toward slight reoxidation of the samples prior to TGA, that the assumed composition $LaNi_{1-x}M_xO_3$ for the reoxidized material is not thermodynamically stable at the chosen $T, p(O_2)$ conditions, or that complete oxidation is only reached asymptotically. For $LaNiO_{2.5}$, TGA shows that the attempted degree of reduction was almost achieved, viz., $LaNiO_{2.517}$. An alternative interpretation of the TGA result would be that complete reduction was achieved, viz., $LaNiO_{2.500}$, whereas the oxidized product had composition $LaNiO_{2.983}$. No iodometric titration for checking the latter possibility was done.

TABLE 1
Oxygen Content and Unit Cell Dimensions for $LaNi_{1-x}M_xO_{2.5+\delta}$ (M = Fe, Co, Mn) at 298 K[a]

Composition	δ	a (Å)	c (Å)	V (Å^3)
$LaNi_{0.90}Mn_{0.10}O_{2.5+\delta}$	0.080	10.846(4)	3.856(2)	453.5(4)
$LaNi_{0.95}Fe_{0.05}O_{2.5+\delta}$	0.055	10.837(1)	3.835(3)	450.3(1)
$LaNi_{0.90}Fe_{0.10}O_{2.5+\delta}$	0.053	10.824(4)	3.871(2)	453.5(3)
$LaNi_{0.90}Co_{0.10}O_{2.5+\delta}$	0.043	10.837(3)	3.836(2)	450.6(3)
$LaNi_{0.875}Co_{0.125}O_{2.5+\delta}$	0.059	10.832(3)	3.837(2)	450.2(1)
$LaNi_{0.75}Co_{0.25}O_{2.5+\delta}$	0.091	10.828(3)	3.863(2)	453.0(2)

[a] Calculated standard deviations are given in parentheses. For oxygen contents, see also the experimental section.

All oxidized and reduced samples were characterized by powder X-ray diffraction (Guinier–Hägg camera, Cu$K\alpha_1$ and Cr$K\alpha_1$ radiation, Si as internal standard) to determine phase purity and sample homogeneity. The X-ray diffraction patterns at 298 K were indexed with the help of the TREOR program (19). Unit cell dimensions were obtained from least-squares refinements using the CELLKANT program (20). Powder X-ray diffraction (PXD) data were collected for the $LaNi_{0.90}M_{0.10}O_{2.5+\delta}$ (M = Fe, Co) samples at the Swiss–Norwegian Beamline BM1 at the European Synchrotron Radiation Facility, Grenoble. X-rays of wavelength 1.09803 Å were obtained by reflection from a Si(111) channel-cut monochromator. The data were recorded in steps of 0.013° in 2θ between 5° and 75° and the counting time per step was 7 s. The fine powder samples were kept in a rotating, 0.3-mm-wide silica glass capillary. The glass capillaries were filled and sealed inside a glovebox. Profile refinement was performed with the GSAS program (21).

Powder neutron diffraction (PND) data were collected for the $LaNi_{0.90}Co_{0.10}O_{2.54}$ sample with the OPUS IV two-axis diffractometer at the JEEP II reactor, Kjeller. Around 10 g of the sample was filled into a cylindrical aluminum sample holder and sealed inside the glovebox. Monochromatized neutrons of wavelength 1.825 Å were obtained by reflection from Ge(111). The scattered intensities were measured by five ^{3}He detectors, positioned 10° apart. Intensity data were collected from $2\theta = 5°$–100° in steps of $\Delta 2\theta = 0.05°$. Profile refinements were performed with the FULLPROF program (22).

X-ray absorption data were recorded for $LaNi_{1-x}M_xO_{2.5+\delta}$ (M = Fe, Co) samples at the Swiss–Norwegian Beamline BM1 at the European Synchrotron Radiation Facility, Grenoble. The samples were diluted and ground with boron nitride (LAB, Merck), pressed into around 1-mm^2 holes in 0.5-mm-thick aluminum disks, and sealed with Kapton tape. The absorption spectra around the iron K-edge at 7.111 keV and the cobalt K-edge at 7.710 keV were recorded in the transmission mode using Ar/N_2-filled ion

chambers. Energy tuning was obtained by means of a Si(111) channel-cut monochromator. A gold mirror was used to reject higher harmonics.

Magnetic susceptibility was measured with a SQUID magnetometer (MPMS; Quantum Design) between 5 and 320 K. The samples were cooled in zero field and measured upon heating in a field of 1 kOe.

RESULTS AND DISCUSSION

Pure $LaNiO_{2.5}$ was found to have a monoclinic structure with $a = 7.836(5)$ Å, $b = 7.809(7)$ Å, $c = 7.469(5)$ Å, and $\beta = 93.96(5)^\circ$ in accordance with reports by Alonso and Martinez-Lope (10). The same type of unit cell was also found for $LaNi_{0.98}Fe_{0.02}O_{2.552}$ with $a = 7.821(9)$ Å, $b = 7.83(2)$ Å, $c = 7.49(1)$ Å, and $\beta = 93.7(1)^\circ$. A new structure type resulted after increased additions of iron to $x = 0.05$ and 0.10 in $LaNi_{1-x}Fe_xO_{2.5+\delta}$. The PXD pattern collected by the Guiner–Hägg film technique was indexed by means of the TREOR program (19) on a tetragonal lattice. The parameters of the tetragonal cell are related to the cubic perovskite cell in the following way: $a_T = 2\sqrt{2}a_C$ and $c_T = a_C$. Upon further increasing the iron content to $x = 0.20$, yet another new phase was found. The tetragonal phase was no longer present, and the tetragonal structure thus exists only in a limited composition region in the $LaNi_{1-x}Fe_xO_{2.5+\delta}$ system, $0.04 \pm 0.01 \leq x \leq 0.15 \pm 0.04$. The tetragonal structure was also found when nickel was substituted by cobalt in the system $LaNi_{1-x}Co_xO_{2.5+\delta}$ for $x = 0.10$–0.25 or by manganese in $LaNi_{0.90}Mn_{0.10}O_{2.5+\delta}$. The compositional region for the tetragonal structure is larger in the cobalt-substituted system than in the iron-substituted system. Only one composition was synthesized in the $LaNi_{1-x}Mn_xO_{2.5+\delta}$ system. The tetragonal cell parameters are given in Table 1, together with the measured oxygen contents of the samples. The cell parameter a_T decreases slightly while c_T increases with increasing Fe or Co content in $LaNi_{1-x}M_xO_{2.5+\delta}$.

The content of the tetragonal unit cell of $LaNi_{1-x}M_xO_{2.50}$ can be described as $La_8(Ni_{1-x}M_x)_8O_{20}$ and has a deficiency of four oxygen atoms relative to eight perovskite-type unit cells, $La_8(Ni_{1-x}M_x)_8O_{24}$. $LaNi_{1-x}M_xO_{2.5+\delta}$ can thus be described as an ordered oxygen-deficient perovskite with, in abbreviated form, an 8–8–20 superstructure. High-resolution PXD data were obtained (Swiss–Norwegian Beamline BM1 at the European Synchrotron Radiation Facility, Grenoble) for the two samples $LaNi_{0.90}M_{0.10}O_{2.5+\delta}$ (M = Fe, Co) to determine the space group and atomic parameters. No systematic extinctions were found in the PXD data, giving the possible space groups $P4$, $P\bar{4}$, $P4/m$, $P422$, $P4mm$, $P\bar{4}2m$, $P4/mmm$, and $P\bar{4}m2$. The space group $P4/m$ was chosen, as the more symmetric space groups were not suitable for a proper placement of all the atoms and the less symmetric space groups gave no significant improvement in the R factors. A neutron diffraction study of $LaNi_{0.90}Co_{0.10}O_{2.54}$ was undertaken to determine the distribution of the oxygen vacancies in the structure. Four weak, extra lines were observed in the neutron diffraction pattern (see Fig. 1),

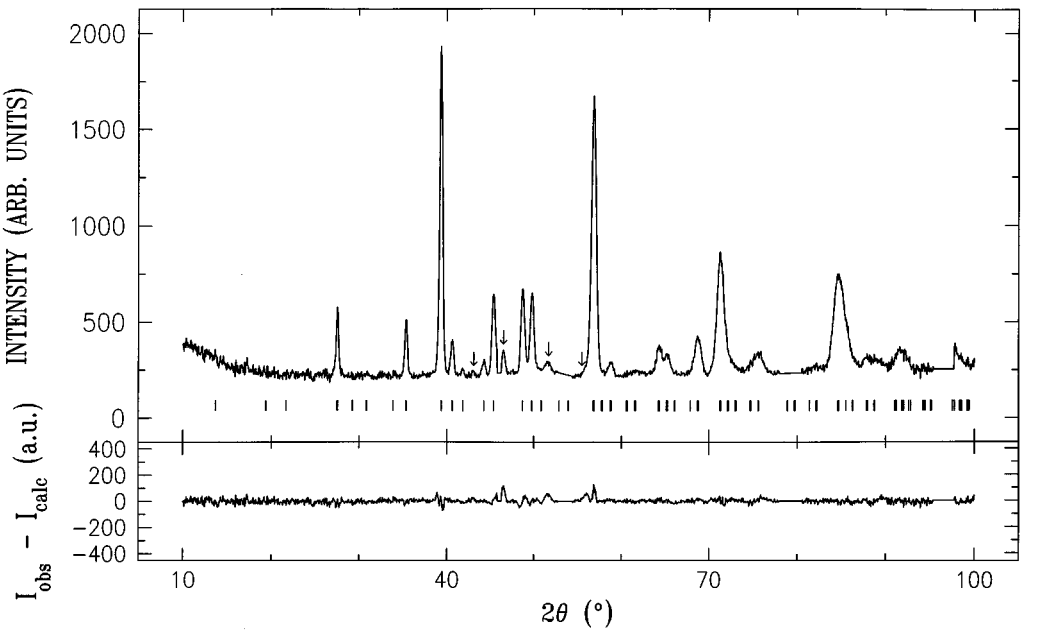

FIG. 1. Observed and difference PND patterns ($\lambda = 1.825$ Å) for $LaNi_{0.90}Co_{0.10}O_{2.54}$ at 298 K. Four weak lines possibly indicating doubling of the c axis are shown by arrows; tentative Miller indices (1, 0, $\frac{3}{2}$), (2, 0, $\frac{3}{2}$), (3, 0, $\frac{3}{2}$), and (4, 0, $\frac{3}{2}$).

TABLE 2
Crystal Data for $LaNi_{0.90}Co_{0.10}O_{2.54}$ at 298 K

Formula	$LaNi_{0.90}Co_{0.10}O_{2.54}$
Formula weight	238.44
Color	dark brown
Space group	$P4/m$
Z	8
λ (Å)	1.825 (neutron), 1.09803 (X-ray)
2θ range	5–100° (neutrons) and 5–75° (X-ray)
Number of reflections	103 (neutron), 221 (X-ray)
Number of structural parameters	21
Profile function	Gaussian (neutron), pseudo-Voigt (X-ray)

	PND	PXD
a_T (Å)	10.835(2)	10.832(1)
c_T (Å)	3.8381(6)	3.8333(5)
V_T (Å^3)	450.6(3)	449.8(2)
R_{wp}	6.25	7.5
R_p	4.57	6.0

which could indicate a possible doubling of the c axis, $c_T = 2a_C$. Crystal data and information on the data collection for $LaNi_{0.90}Co_{0.10}O_{2.54}$ are given in Table 2.

As a starting point for the Rietveld-type refinements, coordinates corresponding to a non-oxygen-deficient cubic perovskite-type structure were chosen. Nickel and cobalt (iron) were assumed to be statistically distributed. Rietveld-type refinements of the PXD pattern using the GSAS program (21) gave refined atomic positions for the metal atoms. The occupancies of the oxygen positions were refined using the FULLPROF program (22) on the basis of PND data. Rapid convergence was obtained, with the occupancy of the oxygen atom O(8) converging to zero. O(8) was therefore completely removed from the model in the final refinements. Models with increased occupation of cobalt on different sets of nickel/cobalt sites all gave slightly higher R factors than the model with statistical distribution of nickel and cobalt over all sites. The refined atomic coordinates are listed in Table 3, and the observed and difference PND and PXD patterns at 298 K are shown in Figs. 1 and 2, respectively.

A projection of the structure of $LaNi_{0.90}Co_{0.10}O_{2.54}$ on the ab plane is shown in Fig. 3. The structure is built up of corner-sharing polyhedra with $(Ni/Co)O_6$ octahedra, $(Ni/Co)O_5$ square pyramids, and $(Ni/Co)O_4$ square-planar groups. Each $(Ni/Co)O_5$ pyramid is linked to one $(Ni/Co)O_4$ group, two $(Ni/Co)O_6$ octahedra, and two $(Ni/Co)O_5$ pyramids along c. To the authors' knowledge, structures with nickel/cobalt simultaneously, in four-, five-, and six-coordinated positions have not previously been reported. However, the structure closely resembles that of $La_{8-x}Sr_xCu_8O_{20}$ ($x = 1.28$–1.92), named the 8–8–20 phase, with CuO_6 octahedra, CuO_5 square pyramids, and CuO_4 square-planar units (14). Distances between the nickel/cobalt and oxygen atoms are given in Table 4. The octahedra are somewhat compressed along the c axis, and the pyramids have four shorter M–O distances (1.84–1.94 Å)

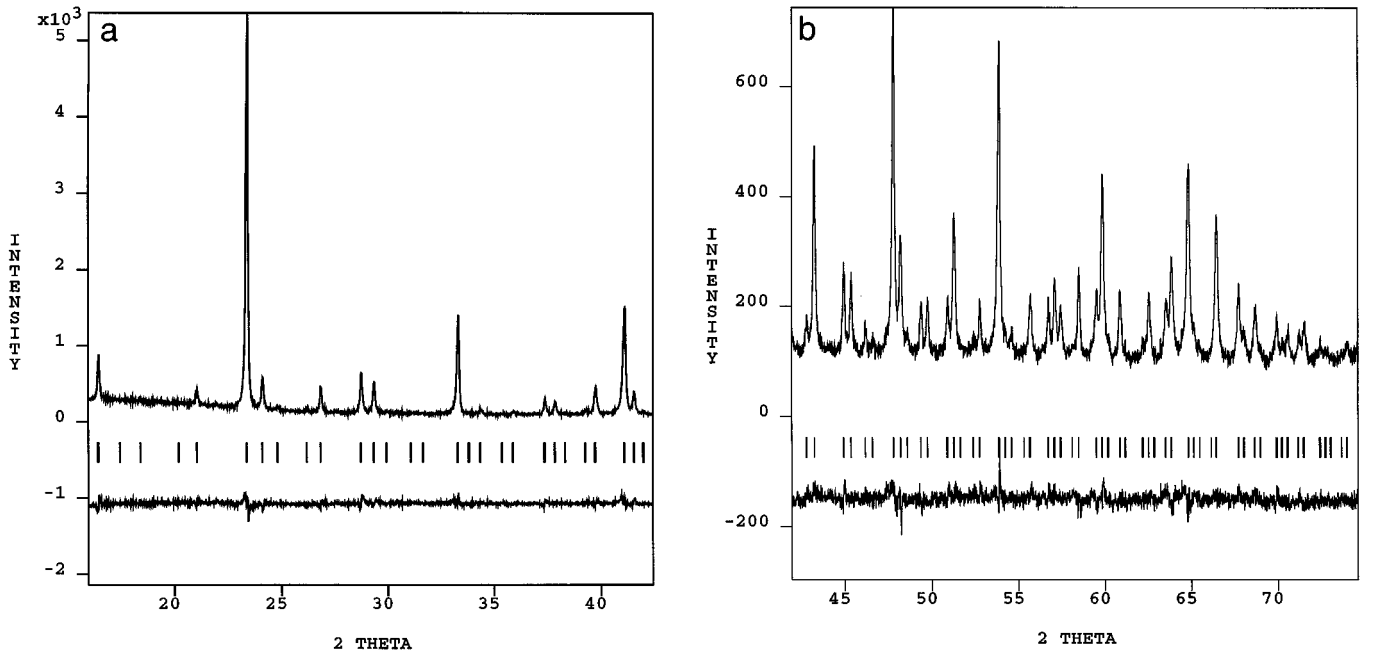

FIG. 2. Observed and difference PXD patterns ($\lambda = 1.09803$ Å) for $LaNi_{0.90}Co_{0.10}O_{2.54}$ at 298 K: (a) $2\theta = 16°$–$42.5°$; (b) $2\theta = 42°$–$76°$. Below $2\theta = 16°$, three weak diffraction peaks were observed at 5.79° (100), 8.21° (110), and 13.02° (210).

TABLE 3
Atomic Coordinates Refined from Powder X-Ray and Neutron Diffraction (in Italics) Data at 298 K for $LaNi_{0.90}Co_{0.10}O_{2.54}$

Atom	Site	x	y	z
La(1)	4*k*	*0.260(3)*	*0.472(2)*	$\frac{1}{2}$
		0.2573(9)	0.4745(8)	
La(2)	4*k*	*0.024(2)*	*0.238(3)*	$\frac{1}{2}$
		0.0287(8)	0.239(1)	
Ni/Co(1)	1*a*	0	0	0
Ni/Co(2)	1*c*	$\frac{1}{2}$	$\frac{1}{2}$	0
Ni/Co(3)	2*c*	0	$\frac{1}{2}$	0
Ni/Co(4)	4*j*	*0.271(2)*	*0.223(2)*	0
		0.279(2)	0.223(2)	
O(1)	1*b*	0	0	$\frac{1}{2}$
O(2)	1*d*	$\frac{1}{2}$	$\frac{1}{2}$	$\frac{1}{2}$
O(3)	2*f*	0	$\frac{1}{2}$	$\frac{1}{2}$
O(4)	4*k*	*0.310(2)*	*0.229(2)*	$\frac{1}{2}$
O(5)	4*j*	*0.162(6)*	*0.095(4)*	0
O(6)	4*j*	*0.382(4)*	*0.880(4)*	0
O(7)	4*j*	*0.395(5)*	*0.344(6)*	0
O(8)[b]	4*j*	*0.368*	*0.091*	0

[a] Space group *P*4/*m*. Calculated standard deviations are given in parentheses. Note position O(8) is vacant.
[b] Occupation zero.

TABLE 4
Interatomic Distances (Å) in $LaNi_{0.90}Co_{0.10}O_{2.54}$ at 298 K[a]

	Octahedral	
Ni/Co(1)–O(1)	×2	1.9166(3)
Ni/Co(1)–O(5)	×4	2.0342(3)
Ni/Co(2)–O(2)	×2	1.9166(3)
Ni/Co(2)–O(7)	×4	2.0369(3)
	Square planar	
Ni/Co(3)–O(3)	×2	1.9166(3)
Ni/Co(3)–O(6)	×2	1.8230(3)
	Square pyramidal	
Ni/Co(4)–O(4)	×2	1.947(5)
Ni/Co(4)–O(5)	×1	1.87(3)
Ni/Co(4)–O(6)	×1	2.439(5)
Ni/Co(4)–O(7)	×1	1.82(3)

[a] Calculated standard deviations are given in parentheses. Type of coordination is given.

and a longer M–O distance (2.43 Å) for the apical oxygen (*trans* to the oxygen vacancy).

In $La_2Ni_2O_5$ the oxygen vacancies are ordered in such a way that square-planar NiO_4 and octahedral NiO_6 units alternate in the *ab* plane along the [110] direction (10). Both kinds of Ni polyhedra are fairly distorted and tilted to optimize the La–O distances, giving rise to a highly strained structure. This may explain why the structure is not particularly stable against small changes in the composition. Substitution of just some 3–10% of the nickel by manganese, cobalt, or iron leads to a new structural arrangement as shown in the present work. The octahedra in $LaNi_{0.90}Co_{0.10}O_{2.54}$ are less distorted than those in $La_2Ni_2O_5$; the variations in the Ni–O distances are 1.917–2.036 and 1.780–2.144 Å, respectively. In the pure cobalt analog of $La_2Ni_2O_5$, $La_2Co_2O_5$, the structure is built up of alternating octahedra and tetrahedra (12). An interesting question concerning $LaNi_{0.90}Co_{0.10}O_{2.54}$ is the local structure for cobalt. A more general question addresses the coordination sites for different *M* substituents (Mn, Fe, Co) in the tetragonal 8–8–20 structure of $LaNi_{1-x}M_xO_{2.5+\delta}$. The square-planar geometry is normally favored by metal ions having

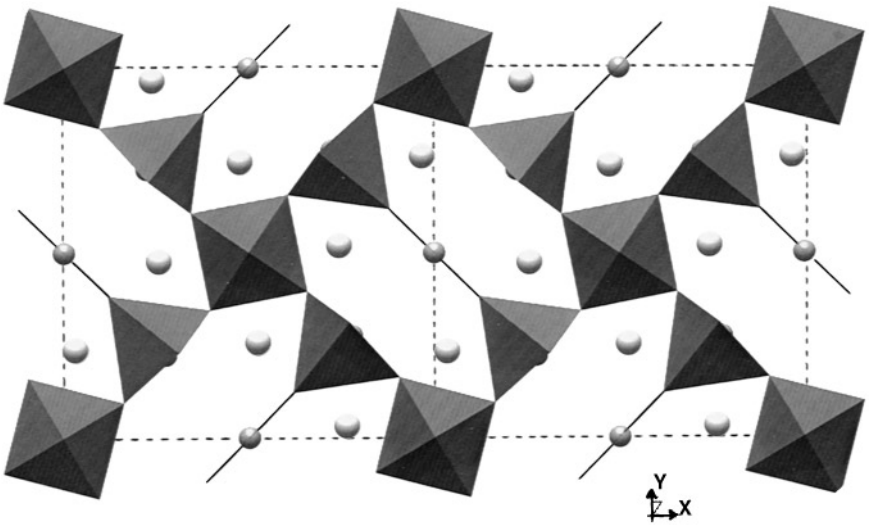

FIG. 3. Crystal structure of $LaNi_{0.90}Co_{0.10}O_{2.54}$ projected on the *ab* plane.

the d^8 configuration (as the Ni^{2+} ion) in a strong field. One could therefore speculate that the nickel ions would occupy the square-planar or square-pyramidal coordination sites and that the substituted cations would prefer the octahedral sites. Indeed a square-planar configuration has not been reported for manganese or iron compounds, whereas a number of square-planar and square-pyramidal compounds are reported for Co(II), Ni(II), and Cu(II). From the refinement of the neutron powder diffraction data of $LaNi_{0.90}Co_{0.10}O_{2.54}$, it was not possible to state in which position the nickel and cobalt ions were located. From the measurement of the oxygen content of the samples, given in Table 1, it can be seen that the oxygen deficiency is slightly less than four atoms per unit cell. The fact that the oxygen deficiency is slightly less than four atoms per unit cell indicates that (most of) the M cations are trivalent. Trivalent M cations and divalent nickel would give an oxygen content of 2.55 ($\delta = 0.05$ in Table 1) for a substitution level $x = 0.10$, i.e., $LaNi_{0.90}M_{0.10}O_{2.55}$. This adds further complexity to the structural model, since the additional oxygen converts locally some square pyramids into octahedra or square-planar units into square pyramids, and the new octahedra may possibly be occupied with the M cation.

To obtain more information on the coordination of the M cation, an X-ray absorption study was performed for M = Fe and Co in $LaNi_{1-x}M_xO_{2.5+\delta}$ (Swiss–Norwegian Beamline BM1 at the European Synchrotron Radiation Facility, Grenoble). XANES spectra for the Fe and Co K-edges in $LaNi_{1-x}M_xO_{2.5+\delta}$ and in $LaCoO_3$ and $LaFeO_3$ are shown in Fig. 4. The Fe and Co ions are trivalent and six-coordinated in the perovskite-type reference compounds. The XANES spectra of the Fe K-edge in the samples and $LaFeO_3$ are similar in shape, which indicates that both the coordination and valency of iron are similar in these compounds. In the iron-substituted oxygen-deficient perovskites $LaNi_{1-x}Fe_xO_{2.5+\delta}$ ($x = 0.05, 0.10$) we therefore propose that iron is trivalent and occupies octahedral positions. This is in agreement with a similar study of iron-substituted $La_{1-x}Sr_xCu_8O_{20}$, where XRD and Mössbauer spectroscopy have been used to show that trivalent iron occupies the octahedral sites (23). The XANES spectra of the Co K-edge of the $LaNi_{1-x}M_xO_{2.5+\delta}$ samples and $LaCoO_3$ are, however, substantially different. This may indicate a difference in the valency and/or the coordination. However, it may also be a reflection of the extraordinary electronic situation in $LaCoO_3$ at 298 K (24), where a mixture of different spin states is assumed to coexist.

The magnetic susceptibility data in Fig. 5 for $LaNi_{1-x}Fe_xO_{2.5+\delta}$ ($x = 0.05, 0.10$) and for $LaNi_{1-x}Co_xO_{2.5+\delta}$ ($x = 0.10, 0.25$) have signatures of magnetic order–disorder transitions. The broad hump around 140 K has also been observed for $La_2Ni_2O_5$ (10), where it was attributed to antiferromagnetic order. For $LaNi_{1-x}Fe_xO_{2.5+\delta}$ the hump shifts from 65 K for $x = 0.05$ to 150 K for $x = 0.10$. For $LaNi_{1-x}Co_xO_{2.5+\delta}$ hardly any hump is visible for $x = 0.10$, possibly a weak anomaly at 135 K, whereas for $x = 0.25$ the low-temperature magnetic transition is clearly shown

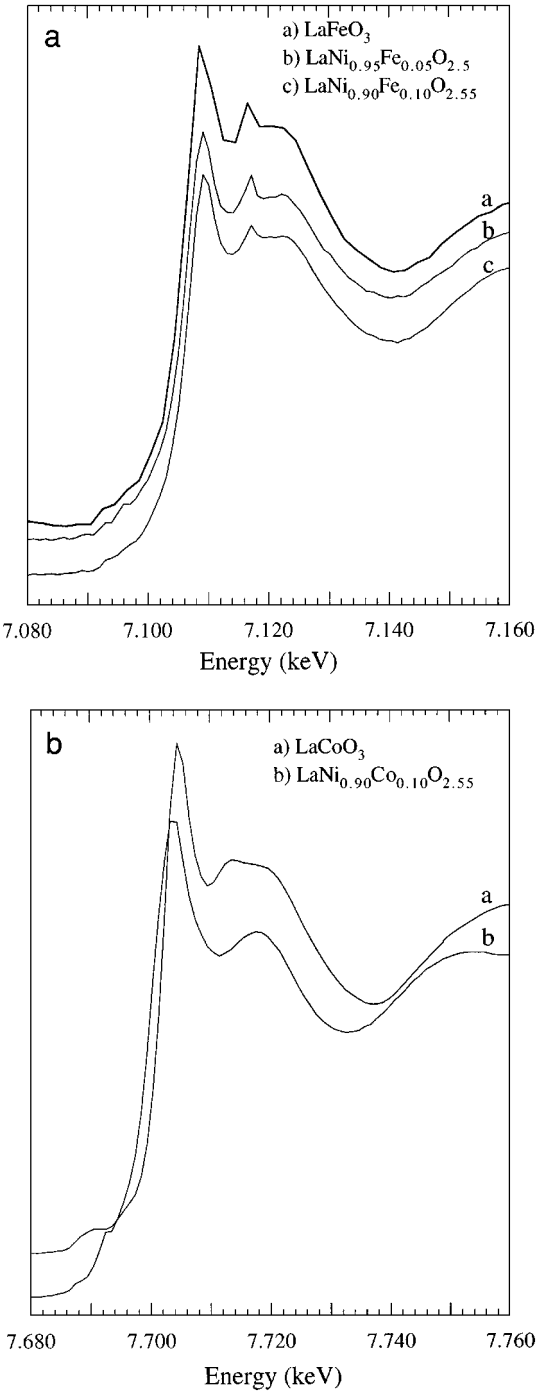

FIG. 4. XANES spectra for the Fe K-edge (A) in $LaNi_{1-x}Fe_xO_{2.5+\delta}$ ($x = 0.05, 0.10$) and $LaFeO_3$ and the Co K-edge (B) in $LaNi_{0.90}Co_{0.10}O_{2.54}$ and $LaCoO_3$.

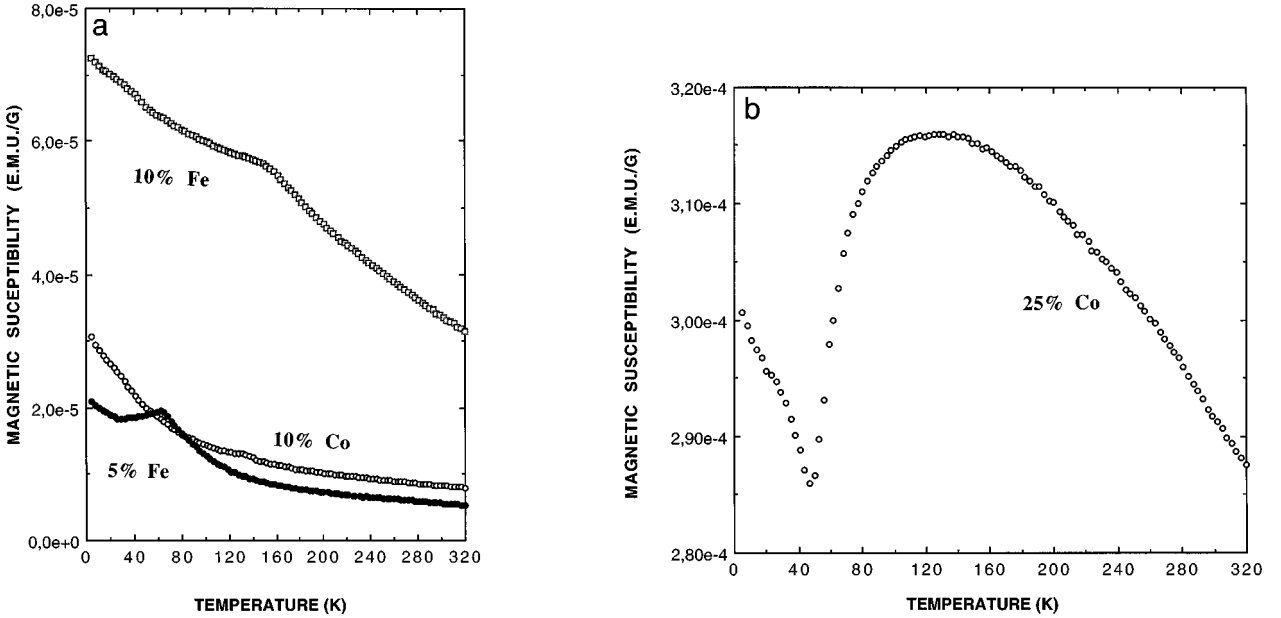

FIG. 5. Magnetic susceptibility data for (a) $LaNi_{0.95}Fe_{0.05}O_{2.555}$, $LaNi_{0.90}Fe_{0.10}O_{2.553}$, and $LaNi_{0.90}Co_{0.10}O_{2.543}$ and (b) $LaNi_{0.75}Co_{0.25}O_{2.581}$.

(Fig. 5). The drop in susceptibility for $x = 0.25$ indicates onset of antiferromagnetic order around 140 K, whereas an order–order transition is indicated by the anomaly around 50 K. Consistent with the almost lacking indications in the magnetic susceptibility of $LaNi_{0.90}Co_{0.10}O_{2.543}$ for magnetic transitions, the PND study revealed no additional peaks of magnetic origin. The $1/\chi(T)$ curves for $LaNi_{0.95}Fe_{0.05}O_{2.555}$ and $LaNi_{0.90}Co_{0.10}O_{2.543}$ are close to linear for $T > 150$ K, the deduced effective paramagnetic moments and Weiss constants being $\mu_{eff} = 2.13\,\mu_B$, $\Theta = 119$ K and $\mu_{eff} = 2.88\,\mu_B$, $\Theta = 214$ K, respectively. For $La_2Ni_2O_5$ the crystallographic structures of Alonso and Martinez-Lope (10) and Moriga *et al.* (8) differ somewhat, mainly owing to different choice of space group ($P2_1/n$ versus $C2/c$) . The structure contains equal amounts of NiO_6 octahedra and NiO_4 square-planar units. Moriga *et al.* suggested Ni^{III} and Ni^{I}, respectively, as the electronic states of nickel (8). As such, both Ni species will carry one unpaired electron (d^7 low spin, d^9), which fits well the experimental value for the effective paramagnetic moment ($1.83\,\mu_B$/Ni observed, $1.73\,\mu_B$/Ni calculated). An evaluation of the likelihood of charge-disproportionated Ni atoms can be made by considering interatomic distances. Choosing 1.654 as the bond strength parameter implies calculated valencies of 2.14 and 2.30 for the square-planar and octahedral Ni atoms in $La_2Ni_2O_5$, far from the values 1 and 3. For the 8–8–20 superstructure, one calculates 2.41, 2.22, and 2.25 for the octahedral, square-pyramidal, and square-planar Ni atoms, respectively. The average is close to that found in $La_2Ni_2O_5$. The substantial deviation from the expected value of two lies in the choice of bond strength parameter. In conclusion, all the nickel atoms appear to be in oxidation state $+II$ in $LaNi_{1-x}M_xO_{2.5+\delta}$.

ACKNOWLEDGMENT

This work has received support from the Research Council of Norway. This paper is Contribution No. 979 from the Swiss–Norwegian Beamline at ESRF.

REFERENCES

1. J. S. Anderson, *in* "Defect and Transport in Oxides" (M. S. Seltzer and R. I. Jaffee, Eds.). Plenum, New York, 1974.
2. "The Chemistry of Extended Defects in Non-metallic Solids" (L. Eyring and M. O'Keeffe, Eds.). North-Holland, Amsterdam, 1970.
3. C. N. R. Rao, J. Gopalakrishnan, and K. Vidyasagar, *Indian J. Chem., Sect. A* **23,** 265 (1984).
4. P. L. Gai and C. N. R. Rao, *Z. Naturforsch., A* **30,** 1092 (1975).
5. M. Crespin, P. Levitz, and L. Gatineau, *J. Chem. Soc., Faraday Trans. 2* **79,** 1181 (1983).
6. P. Levitz, M. Crespin, and L. Gatineau, *J. Chem. Soc., Faraday Trans. 2* **79,** 1195 (1983).
7. K. Vidyasagar, A. Reller, J. Gopalakrishnan, and C. N. R. Rao, *J. Chem. Soc., Chem. Commun.* 7 (1985).
8. T. Moriga, O. Usaka, T. Imamura, I. Nakabayashi, I. Matsubara, T. Kinouchi, S. Kikkawa, and F. Kanamaru, *Bull. Chem. Soc. Jpn.* **67,** 687 (1994).
9. M. J. Sayagués, M. Vallet-Regi, A. Caneiro, and J. M. González-Calbet, *J. Solid State Chem.* **110,** 295 (1994).
10. J. A. Alonso and M. J. Martinez-Lope, *J. Chem. Soc., Dalton Trans.* 2819 (1995).

11. C. N. R. Rao, J. Gopalakrishnan, K. Vidyasagar, A. K. Ganguli, A. Ramanan, and L. Ganapathi, *J. Mater. Res.* **1**(2), 280 (1986).
12. O. H. Hansteen, H. Fjellvåg, and B. Hauback. [to be published]
13. F. Abbattista and M. L. Borlera, *Ceram. Int.* **7,** 137 (1981).
14. L. Er-Rakho, C. Michel, and B. Raveau, *J. Solid State Chem.* **73,** 514 (1988).
15. K. Otzschi, A. Hayashi, Y. Fujiwara, and Y. Ueda, *J. Solid State Chem.* **105,** 573 (1993).
16. K. Otzschi and Y. Ueda, *J. Solid State Chem.* **107,** 149 (1993).
17. K. Otzschi, K. Koga, and Y. Ueda, *J. Solid State Chem.* **115,** 490 (1995).
18. G. Demazeau, A. Marbeuf, M. Pouchard, and P. Hagenmuller, *J. Solid State Chem.* **3,** 582 (1971).
19. P.-E. Werner, "TREOR-5," Institute of Inorganic Chemistry, University of Stockholm, Sweden, 1988. [see also *Z. Kristallogr.* **120,** 375 (1964)]
20. N. O. Ersson, "CELLKANT," Chemical Institute, University of Uppsala, Sweden, 1981.
21. A. L. Larson and R. B. von Dreele, "GSAS, General Structure Analysis System," Los Alamos National Laboratory, Los Alamos, NM, 1994.
22. J. Rodriguez-Carvajal, "FULLPROF," Version 3.0.0, ILL, France, 1995. [unpublished]
23. R. Genouel, C. Michel, N. Nguyen, M. Hervieu, and B. Raveau, *J. Solid State Chem.* **115,** 469 (1995).
24. M. A. Senaris-Rodriguez and J. B. Goodenough, *J. Solid State Chem.* **116,** 224 (1995).